ORIGINAL RESEARCH

Quantitative assessment of device–clot interaction for stent retriever thrombectomy

Kajo van der Marel,[1] Ju-Yu Chueh,[1] Olivia W Brooks,[1] Robert M King,[1] Miklos G Marosfoi,[1] Erin T Langan,[1] Sarena L Carniato,[2] Matthew J Gounis,[1] Raul G Nogueira,[3] Ajit S Puri[1]

▶ Additional material is published online only. To view please visit the journal online (http://dx.doi.org/10.1136/neurintsurg-2015-012209).

[1]Department of Radiology, New England Center for Stroke Research, University of Massachusetts Medical School, Worcester, Massachusetts, USA
[2]Department of Preclinical Science, Stryker Neurovascular, Fremont, California, USA
[3]Emory University School of Medicine/Grady Memorial Hospital-Marcus Stroke and Neuroscience Center, Atlanta, Georgia, USA

Correspondence to
Dr Matthew J Gounis, Department of Radiology, New England Center for Stroke Research, University of Massachusetts Medical School, 55 Lake Ave N, SA-107R, Worcester, MA 01655, USA; matt.gounis@umassmed.edu

KvdM and J-YC contributed equally.

Received 30 November 2015
Revised 30 December 2015
Accepted 4 January 2016
Published Online First 1 February 2016

ABSTRACT

Purpose Rapid revascularization in emergent large vessel occlusion with endovascular embolectomy has proven clinical benefit. We sought to measure device–clot interaction as a potential mechanism for efficient embolectomy.

Methods Two different radiopaque clot models were injected to create a middle cerebral artery occlusion in a patient-specific vascular phantom. A radiopaque stent retriever was deployed within the clot by unsheathing the device or a combination of unsheathing followed by pushing the device (n=8/group). High-resolution cone beam CT was performed immediately after device deployment and repeated after 5 min. An image processing pipeline was created to quantitatively evaluate the volume of clot that integrates with the stent, termed the clot integration factor (CIF).

Results The CIF was significantly different for the two deployment variations when the device engaged the hard clot (p=0.041), but not the soft clot (p=0.764). In the hard clot, CIF increased significantly between post-deployment and final imaging datasets when using the pushing technique (p=0.019), but not when using the unsheathing technique (p=0.067). When we investigated the effect of time on CIF in the different clot models disregarding the technique, the CIF was significantly increased in the final dataset relative to the post-deployment dataset in both clot models (p=0.004–0.007).

Conclusions This study demonstrates in an in vitro system the benefit of pushing the Trevo stent during device delivery in hard clot to enhance integration. Regardless of delivery technique, clot–device integration increased in both clot models by waiting 5 min.

INTRODUCTION

Endovascular treatment of emergent large vessel occlusion (ELVO) using a mechanical approach to thrombectomy has proven clinical benefit.[1–5] As such, research into the mechanics of the embolus that occludes the artery is of fundamental importance.[6 7] Prior studies found that the performance of endovascular ELVO treatment and the risk of distal embolization depend on clot mechanics.[8 9] Recently, thrombectomy with the Trevo stent retriever using a technique that uses forward force to push the device during deployment with spontaneous retraction of the microcatheter has been described, rather than simply unsheathing the device.[10] This technique was associated with a statistically higher rate of first-pass success and higher rates of modified treatment in cerebral ischemia (Thrombolysis In Cerebral Infarction (TICI) 3) reperfusion compared with unsheathing only.

Currently, it is recommended in the instructions for use of some stent retrievers that sufficient time is allotted—estimated at approximately 5 min—for the clot to integrate into the device following deployment. However, in actual clinical practice, the interaction time between clot and device ranges from 30 s to >5 min.[9 11–13] Recently, early loss of immediate reperfusion on angiography during this wait period was found to be associated with a statistically significant increase in the rate of successful recanalization versus cases with persistent reperfusion.[14] This finding suggests that clot embedment into the device facilitates successful thrombectomy.

In this study we measured the interaction between the stent and the clot over time following device deployment. We define the 'clot integration factor' (CIF) as the amount of clot that migrates into the inner volume of the expanded stent. In brief, the CIF is the volume ratio of amount of clot that has penetrated into the stent retriever (numerator) to the total amount of clot forming the occlusion (denominator). In addition, two stent deployment methods (forward pressure on the delivery wire after initial unsheathing vs continuous unsheathing) were compared with a goal of achieving secure clot–device integration.

METHODS

In vitro model

We modified a previously described in vitro model. Briefly, a vascular model was used that included the bilateral internal carotid arteries (ICA) and basilar artery as inputs and the posterior cerebral arteries, A2 and M2 branches as outputs (figure 1). The model included the entire circle of Willis and was manufactured as previously described.[15] Flow sensors (Transonic Systems, Ithaca, New York, USA) measured the ICA, middle cerebral artery (MCA), anterior cerebral artery (ACA) and basilar flow and pressure transducers (Validyne Engineering, Northridge, California, USA) recorded the proximal and distal MCA pressure. Hosecock compressor clamps were used at each outlet to adjust peripheral resistance to maintain physiologically relevant pressure and flow rates (eg, the average MCA flow was 133 mL/min). The working fluid

To cite: van der Marel K, Chueh J-Y, Brooks OW, *et al*. *J NeuroIntervent Surg* 2016;**8**:1278–1282.

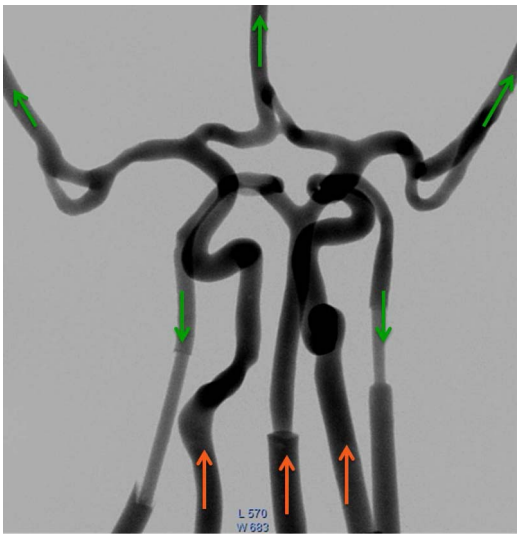

Figure 1 The circle of Willis model used in this study. Bilateral M2 divisions of the middle cerebral arteries and the A2 segments of the anterior cerebral arteries were designed to rejoin distally. In all there were three inputs to the model (red arrows) and four outlets (green arrows).

was maintained at 37°C. To create the ELVO model, two types of clot were introduced into the ICA that migrated with the flow to reliably create an occlusion of the MCA. Hard inelastic clot was generated by thrombin-induced clotting of bovine blood (2.5 NIHU thrombin/mL blood). This clot model is used in the mechanical thrombectomy procedure since it mimics aged cholesterol-rich clot and is prone to fragmentation during thrombectomy.[6] Mixing human blood with thrombin (2.5 NIHU thrombin/mL blood) formed the soft clot model. The composition and mechanical behavior of the soft clot model are similar to those of the fresh red clots commonly found in patients with stroke.[6] In both models a small amount of barium sulfate (1 g/10 mL blood) was added to create contrast necessary for segmentation on CT.

Under fluoroscopic guidance (Allura Xper FD20; Philips, Best, The Netherlands), the Trevo device (Stryker Neurovascular, Fremont, California, USA) was placed across the clot. Immediately following device deployment, a high-resolution cone beam CT was acquired (VasoCT, Philips). After waiting for 5 min following device deployment, imaging was repeated. For each of the two deployment techniques and each of the two clot models, the experiments were repeated eight times resulting in a total of 64 imaging datasets.

Image acquisition and processing

VasoCT images (617 non-binned projections, 20.4 s rotation) were reconstructed at 33% or 50% of the field-of-view (24.7–34.5 mm cube) volume at highest resolution (512^3 isotropic voxels), yielding 48–67 µm resolution.

An image processing pipeline was devised that combines existing geometric (vascular) modeling software (VMTK,[16] ITK, VTK) with in-house developed software. First, anisotropic diffusion filtering was applied to reduce noise. Thereafter, high-intensity shortest paths were traced using Dijkstra's algorithm along user-defined seed points to extract the three marker wires of the device. Uniform cubic B-spline curves were fitted to the extracted paths to obtain smooth wire tracings (figure 2, second image). Next, demarcation of the contrast-enhanced clot was achieved using a threshold-based level-set segmentation algorithm initialized by user-defined seed points near the surface of the clot and morphological closing was applied to the clot segmentation to fill occasional holes (figure 2, third image). Along the three marker wires of the stent, their coordinates were averaged to obtain a device centerline which was subsequently smoothed and used to calculate a reference Frenet frame at each point along the centerline. The interior volume of the device was determined by fitting a Steiner circumellipse through the three closest wire points that intersected each plane orthogonal to the Frenet tangent vector at sequential points along the

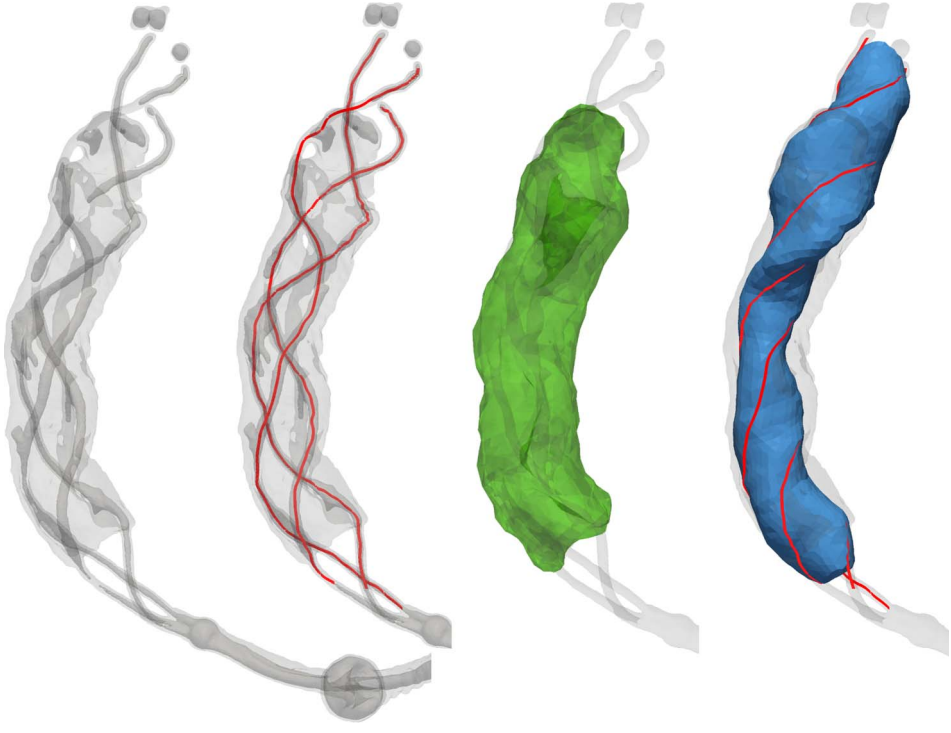

Figure 2 From left to right: Iso-intensity surfaces representing the device were extracted to guide the identification of individual wires. Seed points were manually placed to extract each of the wires (red). Manual seed points were placed to initialize the level-set segmentation of the clot which, after post-processing, was displayed as a surface model (green). Along consecutive points on the centerline, a Steiner circumellipse was fit to the closest points on the three marker wires (red) to model the interior of the device (blue).

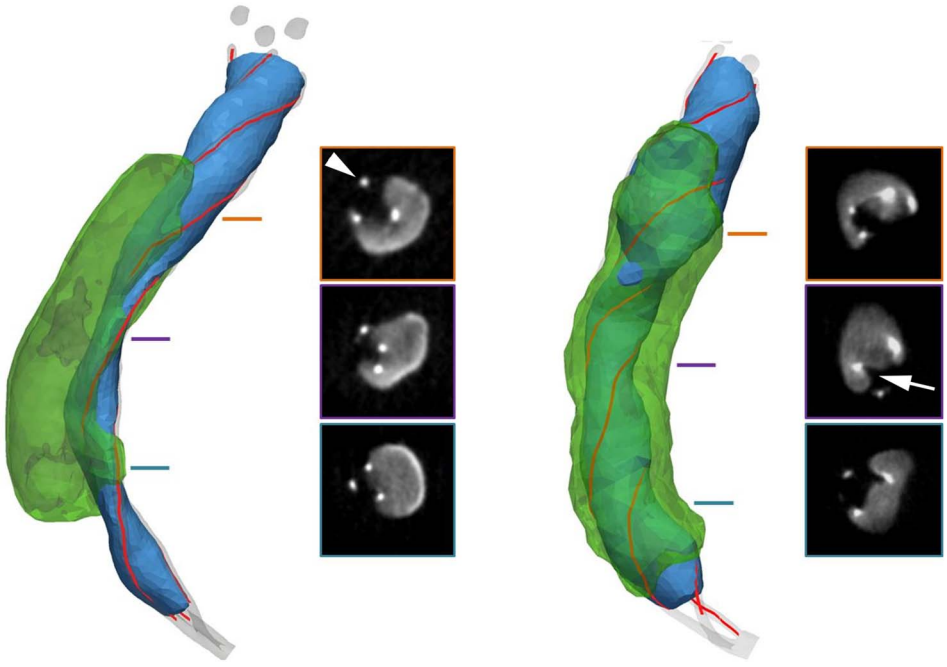

Figure 3 Representative cases in a hard clot model with different Trevo deployment techniques (left, straight unsheathing; right, initial unsheathing followed by pushing the device and spontaneous retraction of the microcatheter). Stent surface shown in blue, clot surface shown in transparent green. Insets show cross-sectional images of the device–clot interaction at different locations along the length of the stent. Sharp focal hyperintensities (arrowhead) are the device marker wires. Note track of stent impregnation into the clot (arrow).

centerline (figure 2, fourth image). Marching cubes and surface re-meshing algorithms were applied to the clot and device segmentations in order to extract and refine appropriate surface model representations for computation of CIF.

CIF was calculated by determining the intersection of the device and clot volumes and subsequently dividing the volume of the intersection by the volume of the clot. Separate two-sample (paired if appropriate) t tests were performed to investigate the effects of deployment technique and time on CIF for different clot models. A p value <0.05 was considered significant.

Clot fragmentation and distal emboli

As previously described, we measured the particle size distribution of clot fragments generated during the thrombectomy in the effluent of the circulation flow loop.[17] All emboli >1000 µm were separated with a pipette and all remaining particles >200 µm were measured using a Coulter counter (Multisizer4; Beckman-Coulter, Brea, California, USA) with a 2000 µm aperture. In each experiment, the total number of clots >200 µm were summed and experimental groups were compared with an ordinary one-way analysis of variance.

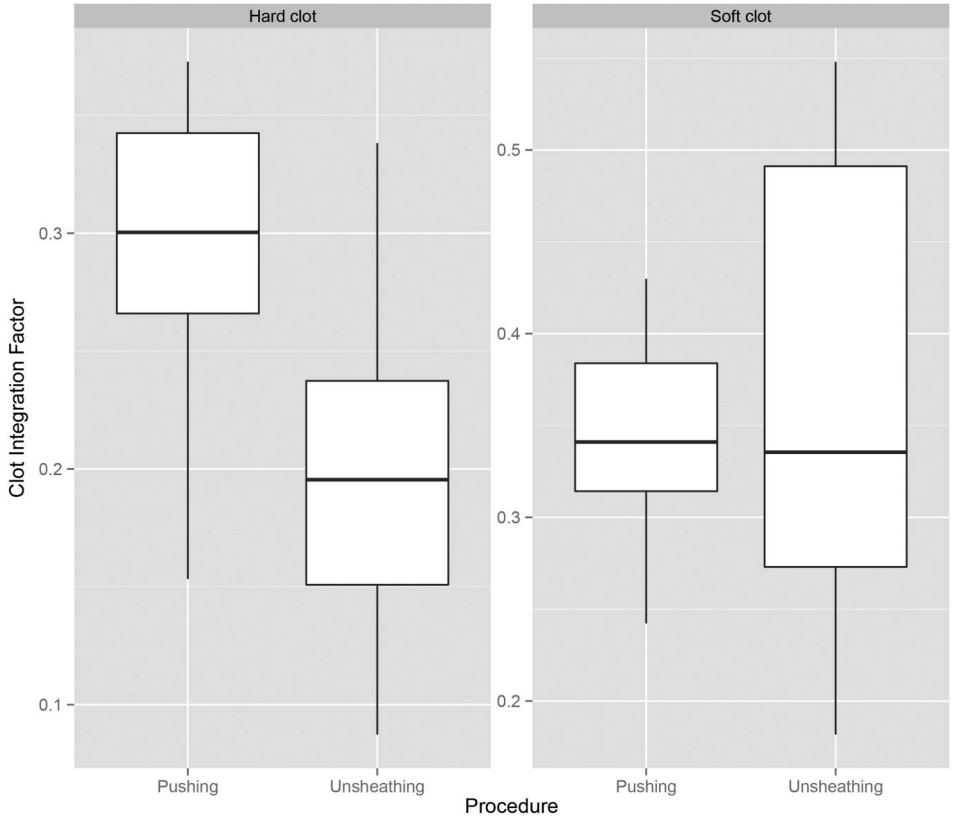

Figure 4 Box plot of the clot integration factor immediately following deployment indicating a significant increase as a function of deployment delivery technique when the device engaged hard clot ($p<0.05$). No significant difference was found in the soft clot model.

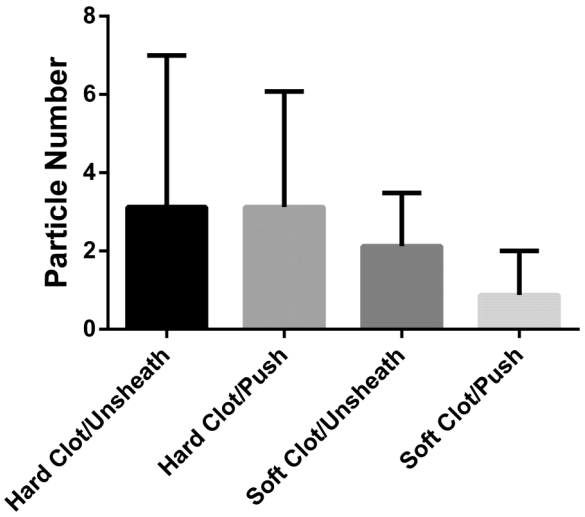

Figure 5 Total number of clot fragments >200 μm for each technique and clot model used.

RESULTS

We were able to use this technique to independently segment the surface of the clot and the stent (figure 3) and calculate the CIF in all cases. In all but three experiments, immediate post-deployment images were available for analysis and final post-deployment data were available for all cases.

First, we investigated the effect of the deployment technique (pushing vs unsheathing) on CIF for the different clot models (figure 4). CIF was significantly different for the two deployment variations when the device engaged hard clot (means: pushing=0.291, unsheathing=0.202; difference between means (95% CI 0.004 to 0.174); t=2.25, df=14; p=0.041) (see online supplementary videos), but not a soft clot model (means: pushing=0.342, unsheathing=0.359; difference between means (95% CI −0.138 to 0.104); t=0.31; df=9; p=0.764). The formation of distal fragments >200 μm did not depend on the technique of retriever deployment (figure 5, p>0.05). Pushing the device and straight unsheathing resulted in a median of 2.5 and 2 hard clot fragments >200 μm per case, respectively. Fewer clot fragments were observed with both techniques in the soft clot model compared with the hard clot model.

Next, we investigated the effect of time on CIF (post-deployment vs final VasoCT) for the different clot models (figure 6). In the hard clot model, CIF increased significantly between post-deployment and final imaging datasets when using the pushing technique (mean difference=0.027 (95% CI 0.006 to 0.047); paired t=3.20, df=6; p=0.019), but not when using the unsheathing technique (mean difference=0.037 (95% CI −0.004 to 0.078); paired t=2.23, df=6; p=0.067). Additionally, there was no significant difference between post-deployment and final runs in the soft clot model using pushing (mean difference=0.053 (95% CI −0.005 to 0.111); paired t=2.18, df=7; p=0.066) or unsheathing (mean difference=0.079 (95% CI −0.010 to 0.168); paired t=2.18, df=6; p=0.072).

We investigated the effect of time on CIF in the different clot models, disregarding the technique. CIF was significantly increased when measured in the final dataset relative to the post-deployment dataset in both the hard clot model (mean difference=0.032 (95% CI 0.012 to 0.051); paired t=3.52, df=13; p=0.004) and in the soft clot model (mean difference=0.065 (95% CI 0.021 to 0.110); paired t=3.13, df=14; p=0.007).

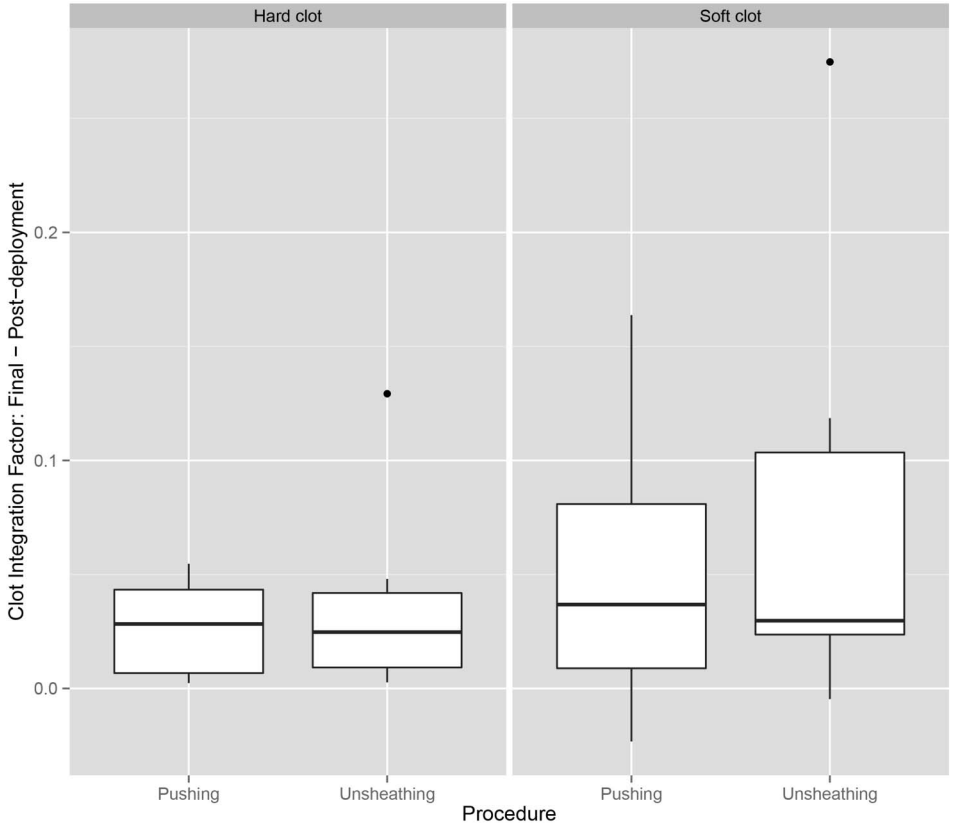

Figure 6 Box plot of the difference in clot integration factor between the post-deployment and final runs in the hard clot and soft clot models showing the effect of time on clot integration. Positive values indicate an increase in clot integration. Outliers are indicated by black dots. There was a small but significant increase overall for both models, and a significant increase in the hard clot model for the pushing but not the unsheathing technique.

DISCUSSION

Previously, the extent of Solitaire expansion in clinical cases using cone beam CT was reported to enable qualitative assessment of occlusion type.[18] In this study, we quantitatively evaluated the integration of the clot into a stent retriever in a controlled in vitro experiment. We chose the Trevo device since it incorporates marker wires into its design that enable us to model the surface of the device separately from the radiopaque clot on VasoCT imaging datasets. Also, this device design (closed-cell, laser cut nitinol tube) allows for expansion of the diameter when forward force is applied. Given the difference in contrast between the clot model and the stent, we could then determine the amount of clot that became enmeshed within the device by measuring the CIF.

The CIF was dependent on delivery technique used in the hard inelastic clot model. By pushing the device during deployment at the level of the clot, more clot integrated within the Trevo without increasing clot fragmentation and distal embolization. However, in this model, simply unsheathing the device led to a decrease in CIF. This may help to explain why pushing the device during delivery is associated with higher rates of first-pass success and TICI 3 results.[10] However, the CIF was independent of the delivery technique in the soft elastic clot.

Another interesting result was that there was a small but significant change in clot integration with the device over time, especially when pushing the device in a hard clot model. Nitinol devices exert a chronic outward force, and it is believed that this force causes the clot to become enmeshed within the device over time as the stent expands through the clot. We could not associate delivery technique with significant changes in CIF over time for the soft clot models within the recommended 5 min observation period. However, when delivery techniques were combined, both soft and hard clot models showed significant increases in CIF over time. Therefore, our model indicates a potential benefit for waiting following deployment of the device, in particular in combination with the pushing technique when engaging a hard clot.

There are several limitations to our study. The clot models used in this study are manufactured in the laboratory and, although designed to mimic the bulk mechanical properties of clinical clot specimens, they are homogenous (unlike clots that cause stroke).[6] Also, our in vitro model uses normal saline as the working fluid and therefore does not model dynamic features of blood, including in situ clot formation or platelet activation. Furthermore, the pushing technique should be carefully performed to avoid forward movement or kinking of the device, which was not observed in any of our experiments. Extending this approach to different devices and clot models is highly dependent on the level of contrast-enhanced clot and radiopaque marker wire visibility and also on the achieved image contrast between the two. If the stent strut attenuation is similar to that of the barium sulfate-enriched clot, segmentation of the device would require additional modeling of its mechanical properties to predict deployment configurations from limited observations outside the clot. Finally, this technique is dependent on device design and can only be used on devices that expand in response to the forward force. It has been reported that the Solitaire device deployed with gentle forward pressure following initial unsheathing is effective in removing migrated coils.[19] Our attempts to measure CIF with the Solitaire device were not successful due to insufficient contrast differences between the device and the clot model.

CONCLUSION

We developed a method to quantitatively measure the amount of clot that integrated with a stent retriever containing radiopaque markers. Clot integration was a function of delivery technique, duration of device implantation, and clot mechanics. This technique could be used in the design and development of future generations of stent retrievers.

Contributors KvdM and J-YC: designed the experiments, performed the experiments, analyzed and processed the data, drafted the manuscript. OWB and RMK: processed the data, revised the draft manuscript. MGM: performed the experiments, revised the manuscript. SLC: designed the experiments, revised the draft manuscript. MJG and RGN: designed the study, revised the draft manuscript. ASP: designed the study, performed the experiments, revised the draft manuscript.

Funding This work was supported by Stryker Neurovascular. Support for imaging systems is provided by Philips Healthcare. The content is solely the responsibility of the authors and does not represent the official views of Stryker or Philips.

Competing interests MJG: Has been a consultant on a fee-per-hour basis for Codman Neurovascular and Stryker Neurovascular; holds stock in InNeuroCo; and has received research support from the National Institutes of Health (NIH), Codman Neurovascular, Stryker Neurovascular, Microvention, Medtronic Neurovascular, Philips Healthcare, InNeuroCo, Neuronal Protection Systems, the Wyss Institute, and Silk Road. SLC: Employed by Stryker Neurovascular. RGN: Stryker Neurovascular (Trevo-2 Trial Principal Investigator—modest; DAWN Trial Principal Investigator—no compensation), Medtronic (SWIFT Trial Steering Committee—modest; SWIFT-Prime Trial Steering Committee—no compensation; STAR Trial Angiographic Core Lab—significant), Penumbra (3D Separator Trial Executive Committee—no compensation), Editor-In-Chief Interventional Neurology Journal (no compensation). ASP: Holds stock in InNeuroCo and has received research grants from Medtronic Neurovascular and Stryker Neurovascular.

Provenance and peer review Not commissioned; externally peer reviewed.

Data sharing statement For access to the raw images obtained in this study, please contact the corresponding author.

REFERENCES

1 Saver JL, Goyal M, Bonafe A, *et al*. Stent-retriever thrombectomy after intravenous t-PA vs. t-PA alone in stroke. *N Engl J Med* 2015;372:2285–95.
2 Goyal M, Demchuk AM, Menon BK, *et al*. Randomized assessment of rapid endovascular treatment of ischemic stroke. *N Engl J Med* 2015;372:1019–30.
3 Berkhemer OA, Fransen PS, Beumer D, *et al*. A randomized trial of intraarterial treatment for acute ischemic stroke. *N Engl J Med* 2015;372:11–20.
4 Campbell BC, Mitchell PJ, Kleinig TJ, *et al*. Endovascular therapy for ischemic stroke with perfusion-imaging selection. *N Engl J Med* 2015;372:1009–18.
5 Jovin TG, Chamorro A, Cobo E, *et al*. Thrombectomy within 8 hours after symptom onset in ischemic stroke. *N Engl J Med* 2015;372:2296–306.
6 Chueh JY, Wakhloo AK, Hendricks GH, *et al*. Mechanical characterization of thromboemboli in acute ischemic stroke and laboratory embolus analogs. *AJNR Am J Neuroradiol* 2011;32:1237–44.
7 Luo ZH, Chung A, Choi G, *et al*. Creation of fibrinogen-enhanced experimental blood clots to evaluate mechanical thrombectomy devices for treatment of acute stroke: an in vitro study. *J Vasc Interv Radiol* 2012;23:1077–83.
8 Chueh JY, Kühn AL, Puri AS, *et al*. Reduction in distal emboli with proximal flow control during mechanical thrombectomy: a quantitative in vitro study. *Stroke* 2013;44:1396–401.
9 Park H, Hwang GJ, Jin SC, *et al*. A retrieval thrombectomy technique with the Solitaire stent in a large cerebral artery occlusion. *Acta Neurochir (Wien)* 2011;153:1625–31.
10 Haussen DC, Rebello LC, Nogueira RG. Optimizating clot retrieval in acute stroke: The push and fluff technique for closed-cell stentrievers. *Stroke* 2015;46:2838–42.
11 Broussalis E, Trinka E, Hitzl W, *et al*. Comparison of stent-retriever devices versus the Merci retriever for endovascular treatment of acute stroke. *AJNR Am J Neuroradiol* 2013;34:366–72.

12 Mendonça N, Flores A, Pagola J, *et al*. Trevo versus solitaire a head-to-head comparison between two heavy weights of clot retrieval. *J Neuroimaging* 2014;24:167–70.
13 Soize S, Kadziolka K, Estrade L, *et al*. Mechanical thrombectomy in acute stroke: prospective pilot trial of the solitaire FR device while under conscious sedation. *AJNR Am J Neuroradiol* 2013;34:360–5.
14 Okawa M, Tateshima S, Liebeskind D, *et al*. Early loss of immediate reperfusion while stent retriever in place predicts successful final reperfusion in acute ischemic stroke patients. *Stroke* 2015;46:3266–9.
15 Chueh JY, Wakhloo AK, Gounis MJ. Neurovascular modeling: small-batch manufacturing of silicone vascular replicas. *AJNR Am J Neuroradiol* 2009;30:1159–64.
16 Antiga L, Piccinelli M, Botti L, *et al*. An image-based modeling framework for patient-specific computational hemodynamics. *Med Biol Eng Comput* 2008;46:1097–112.
17 Chueh JY, Puri AS, Wakhloo AK, *et al*. Risk of distal embolization with stent retriever thrombectomy and ADAPT. *J Neurointerv Surg*. Published Online First: 24 Dec 2014. doi: 10.1136/neurintsurg-2014-011491
18 Mitchell BD, Chinnadurai P, Chintalapani G, *et al*. Endovascular recanalization in acute ischemic stroke using the solitaire FR revascularization device with adjunctive C-arm CT imaging. *AJNR Am J Neuroradiol* 2015;36:1317–20.
19 Leslie-Mazwi TM, Heddier M, Nordmeyer H, *et al*. Stent retriever use for retrieval of displaced microcoils: a consecutive case series. *AJNR Am J Neuroradiol* 2013;34:1996–9.